ELSEVIER

Lithos 48 (1999) 57–80

LITHOS

Imaging the continental upper mantle using electromagnetic methods

Alan G. Jones

Geological Survey of Canada, 615 Booth St., Room 218, Ottawa, Ontario, Canada K1A 0E9

Received 27 April 1998; received in revised form 11 November 1998; accepted 20 November 1998

Abstract

The internal structure of the continental lithosphere holds the key to its creation and development, and this internal structure can be determined using appropriate seismic and electromagnetic methods. These two are complementary in that the seismic parameters usually represent bulk properties of the rock, whereas electrical conductivity is primarily a function of the connectivity of a minor constituent of the rock matrix, such as the presence of a conducting mineral phase, e.g. carbon in graphite form, or of a fluid phase, e.g. partial melt or volatiles. In particular, conductivity is especially sensitive to the top of the asthenosphere, generally considered to be a region of interconnected partial melt. Knowledge of the geometry of the lithosphere/asthenosphere boundary is important as this boundary partially controls the geodynamic processes that create, modify, and destroy the lithosphere. Accordingly, collocated seismic and electromagnetic experiments result in superior knowledge than would be obtained from using each on its own. This paper describes the state of knowledge of the continental upper mantle obtained primarily from the natural-source magnetotelluric technique, and outlines how hypotheses and models regarding the development of cratonic lithosphere can be tested using deep-probing electromagnetic surveying. The resolution properties of the method show the difficulties that can be encountered if there is conducting material in the crust. Examples of data and interpretations from various regions around the globe are discussed to demonstrate the correlation of electromagnetic and seismic observations of the lithosphere–asthenosphere boundary. Also, the observations from laboratory measurements on candidate mineralogies representative of the mantle, such as olivine, are presented.

Keywords: Electrical conductivity; Upper mantle property; Mantle anisotropy

1. Introduction

Knowledge of the internal structure of the lithosphere and the geometry of the lithosphere–asthenosphere boundary are critically important for developing our understanding of the dynamics of the Earth. Models of lithospheric growth proposed by different authors are based on differing hypotheses, and many of these hypotheses are unfettered by constraints. Similarly, geodynamic models of mantle flow generally assume a simplistic geometry for the lithosphere–asthenosphere boundary, whereas topography on this boundary has significant implications for such flow models, as shown in the paper by De Smet et al. (1999, this issue). Deductions about the depth-variation of appropriate physical parameters through-

0024-4937/99/$ - see front matter
PII: S0024-4937(99)00022-5

out the whole of the lithosphere and into the asthenosphere can be used to constrain these hypotheses and models.

Evolutionary models of lithospheric growth of continental roots by Jordan (1988) and Ashwal and Burke (1989) appeal to uniformitarianism, and advance modern-day processes as explanations of tectonic events that occurred since the Earth formed. Jordan (1988) suggested that repeated cycles of differentiation and collisional thickening lead to a mantle root, whereas Ashwal and Burke (1989) proposed that cratons are formed by assembling collided island arcs composed of depleted mantle material. In contrast, Helmstaedt and Schulze (1989) suggested more buoyant subduction occurred during the Archean, as a consequence of higher spreading rates, leading to continental roots being formed by imbrication of shallowly subducted slabs. Kusky (1993) modified this model by incorporating trapped wedges of fertile mantle within the stack of imbricated slabs. Models of growth by non-tectonic processes are those of Thompson et al. (1996), who proposed that lithosphere thickened slowly by basal accretion of mobile asthenospheric material, and Polet and Anderson (1995), who hypothesized that permanent roots beneath old cratons may be quite small, and that cold downwelling in the asthenosphere induced by them increases their apparent size and depth. Hoffman (1990) discussed some of these models, and their implications, for the root of the Canadian shield part of the North American craton, concluding that the existing geological data are not adequate for discriminating between the various models, nor can the data define new models that can explain the origin of deep cratonic roots. The apparent Precambrian age of the root is compatible with the Helmstaedt and Schulze (1989) model, but not with either the Jordan (1988) or Ashwal and Burke (1989) result, and is disputed by Thompson et al. (1996) and Polet and Anderson (1995). All of these models have different physical characteristics that can be tested with appropriate geophysical data, and clearly new data are required to further our understanding of the roots of the continents.

Unfortunately, there are but two geophysical techniques that can measure physical parameters of the lithosphere. Whereas the density and thermal parameters are inferred using gravity and geothermics, the seismic wave parameters and electrical conductivity can be measured, albeit through spatially-averaging filters, with appropriate surface-based methods. Since the early 1990s, there has been an explosion in the numbers of teleseismic observations, and some limited attempts using controlled-source seismology, for lithospheric mantle studies. In contrast, the electromagnetic (EM) community was studying the submantle lithosphere in the 1970s and early-1980s, but since the mid-1980s the focus has been more on the crust. This emphasis was due, in the main, to improved instrumentation and time series processing methods for higher frequency data concurrent with global research thrusts and the program directions of the major funding agencies.

Recent development of stable and highly-sensitive (30 pT and lower noise levels) magnetometers for long period measurements, coupled with a renewal of scientific interest in the sub-crustal lithosphere, have resulted in a number of high-quality deep-probing EM experiments being carried out in the last few years. The results of most of these though have yet to be published.

This paper will briefly review the principles of EM appropriate for imaging the Earth, and describes the natural-source magnetotelluric (MT) method. Some results for the lithosphere and asthenosphere are discussed under the categories of (i) continental lithospheric mantle resistivity, (ii) electrical asthenosphere, (iii) deep mantle observations, and (iv) mantle electrical anisotropy. Laboratory conductivity studies on mantle rocks are presented, together with some discussion of the correlation of electrical and seismic asthenospheres. Conclusions discuss the various hypotheses for lithospheric growth and possible tests using appropriate EM data.

2. Principles of electromagnetism

2.1. Electromagnetic propagation

The propagation of an electromagnetic (EM) wave through a uniform homogeneous medium is governed by the *propagation constant*, k, given by

$$k^2 = \omega\mu(i\sigma - \omega\epsilon)$$

where ω is the radial frequency of oscillation, μ is the magnetic permeability, σ is the electrical con-

ductivity and ϵ is the electric permittivity. Accordingly, the physical parameters being sensed in any electromagnetic experiment are electrical conductivity and electric permittivity (analogous to magnetic susceptibility) within a volume of physical dimension given by an inductive scale length at frequency ω.

For most Earth materials, at frequencies less than a few tens of thousands of Hertz, the contribution from the second term in the equation, $\omega^2\mu\epsilon$, which describes the *displacement currents* deduced by James Clerk Maxwell in the 1860s, can be ignored as it is many orders of magnitude smaller than the first term, $\omega\mu\sigma$, which describes the flow of *conduction currents*. Once displacement currents are ignored from the wave equations, the equations reduce to familiar diffusion equations met in other branches of geophysics (e.g., gravity, heat flow), with the important difference that they are vector diffusion equations, not scalar ones. General solutions to the vector diffusion equations are given by linear combinations of elementary solutions describing exponential decay within the medium.

In a uniform medium, a measure of the inductive scale length is given by the *skin depth*, δ, which is the distance by which the amplitude is $1/e$'th of its initial value, given by

$$\delta = \sqrt{\frac{2}{\omega\mu\sigma}} \ [\mathrm{m}]$$

which reduces to

$$\delta = 0.503\sqrt{\rho T} \ [\mathrm{km}]$$

where ρ is the electrical resistivity (in Ω m), given by $1/\sigma$, and T is the period of oscillation (in s), given by $2\pi/\omega$. Accordingly, with electromagnetic methods penetration to all depths is assured from the skin depth phenomenon — one merely needs to measure at lower and lower frequency (longer and longer period) to probe deeper and deeper into the Earth.

2.2. Conduction types

There are two dominant types of conduction currents in the crust and upper mantle: *electronic conduction* and *ionic conduction.*

Electronic conduction (electrons or polarons as charge carriers) is the dominant conduction mechanism in most solid materials, and is a thermally-activated process governed by the appropriate activation energy for the material, Boltzmann's constant, and the absolute temperature.

Ionic conduction (ions as charge carriers) is the dominant conduction mechanism in fluids, but is also important for olivine at high temperatures (1100–1200°C).

2.3. Mental manipulation

The controlling physical parameter in most EM surveys is the electrical conductivity of the medium, σ. Its inverse, electrical resistivity ρ, is more often discussed in the literature, mainly because the values of conductivity are small fractions, and thus less easy to work with. However, the physical laws are governed by the connectivity of a conducting component within the medium, and so literature from laboratory measurements on rocks is usually in conductivity. Also many of the forward and inverse algorithms are based on the variation of conductivity with depth and lateral distance. This duality is akin to slowness and velocity in seismic studies.

An additional complication for the recreational peruser of EM literature is that data are presented in terms of variation with frequency or period, and sometimes both in the same publication, depending on the periodicity of the exciting external wave field and the problem being investigated. Generally, if the depth of interest is in the near surface, then the data will be presented in terms of decreasing frequency, from kiloHertz to Hertz, whereas for deeper studies they will be presented in terms of period, from seconds to thousands of seconds. In this publication period is used exclusively.

2.4. Electrical resistivity

The electrical resistivity of Earth materials varies by more orders of magnitude than any other physical parameter with the exception of viscosity, from one million ohm-metres (10^6 Ω m) for a competent unfractured batholith to one millionth of an ohm-metre (10^{-6} Ω m) for the most conducting sulphides and graphite. Sea water has a resistivity of 0.3 Ω m,

and highly saline brines can be as low as 0.005 Ω m (Nesbitt, 1993). Typical ranges of values for certain rock types and for some conducting phases (saline fluid or graphite film) are given in Fig. 1. The bulk electrical resistivity observed from the surface varies over a far smaller range, typically from 1 Ω m to 10^4 Ω m, due to the limited resolving power of the diffusive technique. However, even this reduced range of four orders of magnitude makes EM far more sensitive to the presence of anomalies than most other geophysical techniques.

The bulk conductivity of a medium is governed by the amount and interconnectivity of the conducting phase, which is usually a very minor constituent of the rock matrix. Archie's Law is often appropriate as a first-order model for the total conductivity of a medium

$$\sigma_m = \sigma_f \eta^n$$

where σ_m and σ_f are the conductivities of the bulk medium and the fluid (conducting) phase, respectively, η is the porosity, and the exponent n has a value between 1 and 2. The host rock conductivity, σ_r, is assumed to be sufficiently low to have little effect. Other estimates for the conductivity of a two-phase mixture are given by serial and parallel network analogues (Madden, 1976, 1983; Bahr, 1997) and by the Hashin and Shtrikman (1963) bounds. These latter bounds find application in many branches of geophysics, including effective transport properties of two-phase mixtures and the pressure dependence of elastic constants, and the Hashin–Shtrikman upper bound is identical to the one of Maxwell (1892) for widely-dispersed spheres embedded in a fluid.

3. The method — magnetotelluric sounding

Hjelt and Korja (1993) compare and contrast the various electromagnetic methods used for imaging the Earth's crust and upper mantle, stressing the ''zooming'' ability of EM from lithospheric scale structures (hundreds of kilometres) to small, near-surface local scale structures (metres length scale). The natural source magnetotelluric (MT) method is the most appropriate electromagnetic technique for probing into the deep lithosphere of the continents. Controlled-source EM surveys require a very large

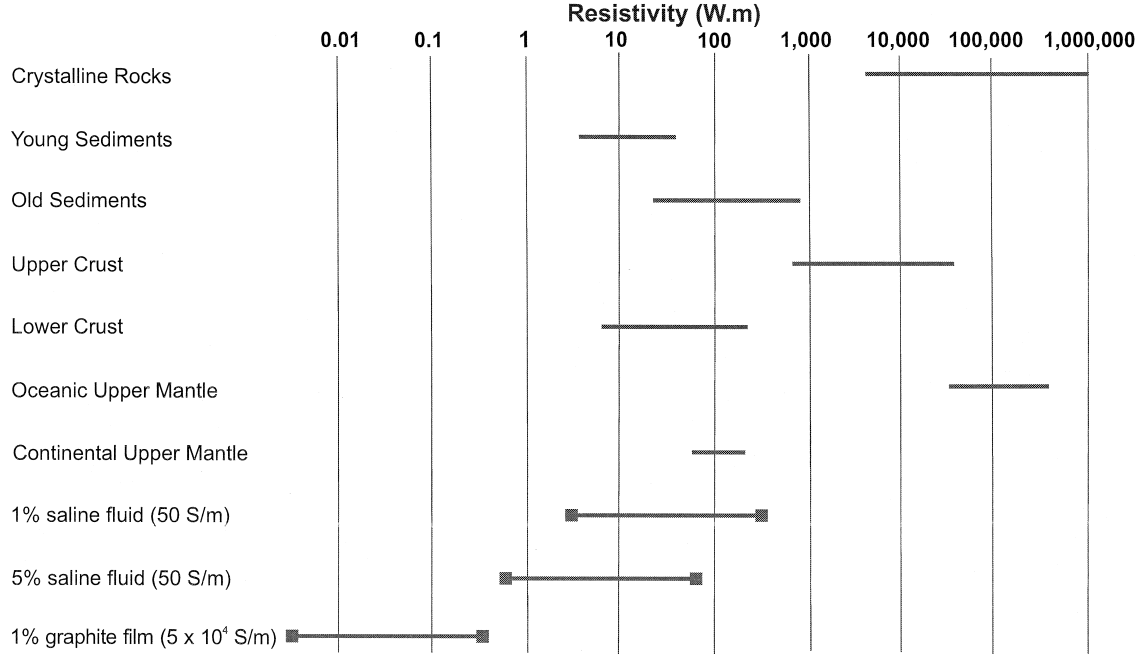

Fig. 1. Resistivity ranges for Earth materials.

source to penetrate to depths greater than the middle crust, and has only been done on relatively few occasions. Most of these surveys used power lines, such as the 1200-km-long Cabora Bassa powerline in southern Africa before it came into service (Blohm et al., 1977), the Sierra Nevada DC power line (Lienert, 1979), and the 180-km-long line between Finland and Sweden (Kaikkonen et al., 1996). Constable et al. (1984) used a 200-km-long telephone line. A unique deep-probing controlled source was provided by the huge Kibliny magneto-hydrodynamic generator on the Kola peninsula used by the Russians for underwater communication to submarines around the globe (Velikhov et al., 1986, 1987; Heikka et al., 1984). Problems with logistics and the necessity of dealing with source geometry hamper such work for imaging deep into the mantle.

In contrast, the MT method uses the time-varying Earth's magnetic field as its source, and depth penetration is assured. The variations are caused by the interaction of the solar plasma with the Earth's magnetosphere. By Faraday's Law of Induction, this varying magnetic field induces an electric current, and the current generates an electric (called ''telluric'') field in the Earth, and the strength of the telluric field is dependent on the conductivity of the medium. Hence, by observing the magnetic and electric fields simultaneously, and determining their ratios at varying frequencies (equivalent to depths by the skin depth phenomenon), one can derive the conductivity variation with both depth and distance. It can be shown that for a one-dimensional Earth, if one has perfect data at all frequencies there exists only one model that will fit the data (Bailey, 1970; Weidelt, 1972). This uniqueness theorem separates MT from other potential field methods with non-uniqueness as an inherent property. Whereas it is, of course, never possible to obtain perfect data, the existence of this uniqueness theorem propels MT people to make more and more accurate and precise estimates of the Earth responses.

On the surface of the Earth, one measures the time variations of the three components of the magnetic field, and the two horizontal components of the Earth's electric field. An example of their variation over a 24-h period is shown in Fig. 2 from a site in northern Canada (within the Yellowknife seismic array) for 12th January, 1997 (UT). Local magnetic midnight (based on geomagnetic coordinates, rather than geographic ones) at Yellowknife is at approxi-

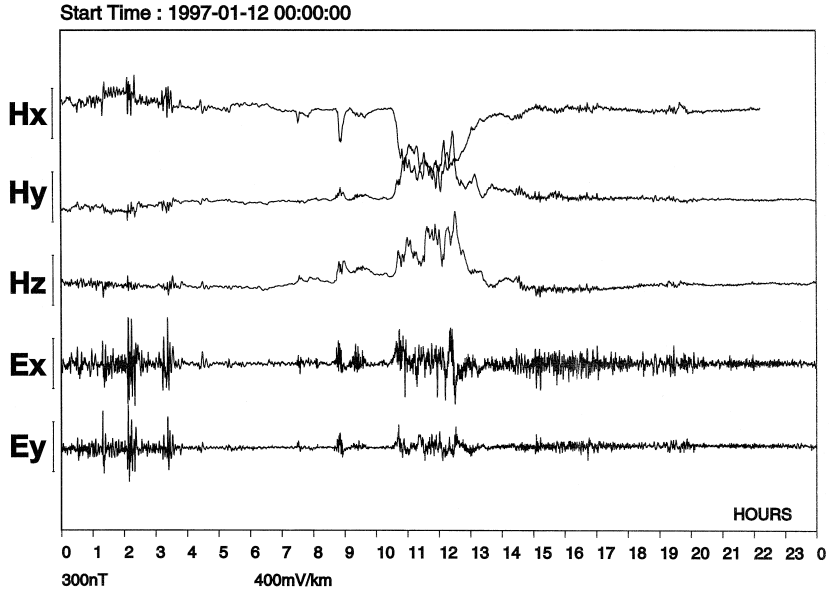

Fig. 2. Typical magnetotelluric time series. Shown are the time variations of one day of data (12 January 1997, Universal Time) recorded at an MT site at Yellowknife, northern Canada. The scale bar of the three magnetic components represents 300 nT, and the scale bar for the two horizontal electric components represents 400 mV/km.

mately 09:00 UT (01:00 local time), when there is a strong negative excursion of *Hx*. Two hours later is a substorm event rich in long period activity, followed by high signal activity at shorter periods.

From the ratios of any two field components in the frequency domain, one can define a complex *impedance*, $Z_{xy}(\omega)$, at radial frequency ω between, e.g., the northward-directed electric field $E_x(\omega)$ and the perpendicular eastward-directed magnetic field component $H_y(\omega)$, from

$$Z_{xy}(\omega) = \frac{E_x(\omega)}{H_y(\omega)},$$

and the S.I. units of Z are ohms. The ratios of the powers of the fields can be scaled as an *apparent resistivity*, akin to DC resistivity exploration,

$$\rho_{a,xy}(\omega) = \frac{1}{\omega\mu}\left|\frac{E_x(\omega)}{H_y(\omega)}\right|^2,$$

and the phase lead of the electric field over the magnetic field is given by

$$\phi_{xy}(\omega) = \tan^{-1}\left(E_x(\omega)/H_y(\omega)\right).$$

Over a half-space, the apparent resistivity gives the true resistivity of the half space at all frequencies, and the phase is 45°. For a multi-layered Earth, the two parameters vary with frequency, and their variation with frequency can be inverted to reveal the structure. Examples of the apparent resistivity and phase curves for some layered Earth models are given below.

4. Continental lithospheric mantle resistivity

We know, from ocean-bottom controlled-source EM experiments, that the uppermost oceanic mantle is highly resistive, of the order of 10^5 Ω m (Cox et al., 1986). This value is consistent with laboratory measurements on dry olivine and peridote. However, estimates of the resistivity of the continental lithospheric mantle are far lower, typically from 80–200 Ω m. A problem with determining this resistivity correctly is that the resistive lithospheric mantle is usually sandwiched between two conducting layers, the lower crust and the electrical asthenosphere, and thus we can only obtain a minimum bound on its value as in 1D the MT method is generally insensitive to the actual resistivity of resistive layers.

Generating the forward response of an Earth model, comprising a reference model with a conducting lower crust and an asthenospheric region (see below for description), and adding a small amount of random scatter and noise (2% to apparent resistivities and 0.58° to phase), we can invert the model data to examine the resolution capabilities in such situations. Fig. 3 shows the data, the theoretical model, and the smoothest model and a seven-layer model that fit the data to a normalized root-mean-square (RMS) misfit of one, i.e., these models neither underfit nor overfit the data and their errors, but fit to within exactly one standard error on average. Clearly, the true resistivity of the uppermost lithospheric mantle is not well resolved, as shown by the gross underestimate of the smooth model just below the base of the crust and by the very large value for the seven-layer model. This lack of resolution is confirmed by singular value decomposition sensitivity analysis (e.g., Jones, 1982) of the seven-layer model which demonstrates that of the 13 parameters (model parameters are the seven layer resistivities and six thicknesses; eigen parameters are combinations of these), nine are well resolved. The weakly-resolved parameters are the resistivity-thickness of the fourth layer (asthenosphere), the resistivity of the first layer (upper crust), and a mixture of model parameters of the third and fifth layers. The worst-resolved parameter is the resistivity of the third layer (the uppermost lithospheric mantle above the asthenosphere), with an error of over an order of magnitude. Thus, there is no resolution in even such high quality data to the actual resistivity of the uppermost mantle — we can only set a minimum bound on it. Its thickness, however, is one of the most well-resolved of the model parameters (third-best resolved, error of 0.5%), as it separates the two conducting zones and the amount of separation greatly affects the response. This means that although we cannot usually know the actual resistivity of the continental lithospheric mantle, we can know its thickness well, so can estimate the depth to any electrical asthenosphere.

Whereas the existence of a conducting lower crust used to be thought of as anomalous, quite to the

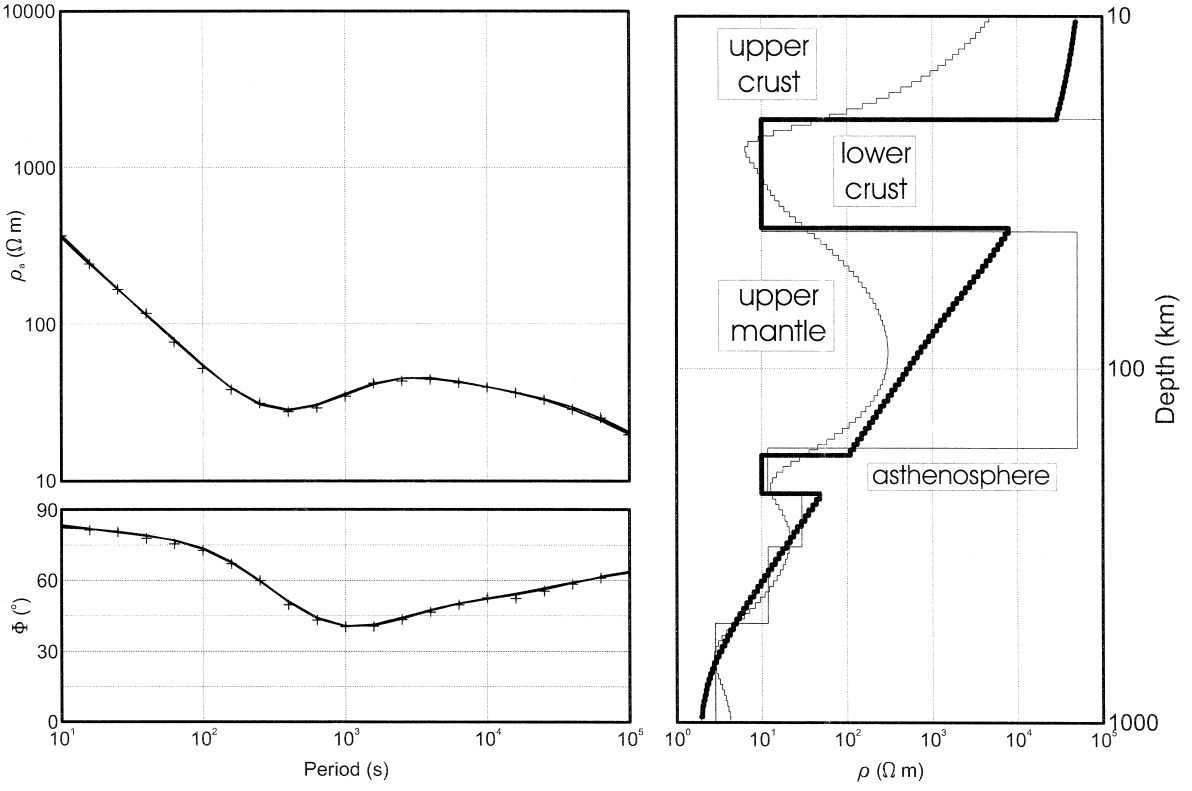

Fig. 3. Synthetic data (with 2% scatter and error) generated from a theoretical reference model containing a lower crustal conductor and an asthenospheric zone (heavy line). The two other models, one a smooth inversion and the other a 7-layer inversion, fit the synthetic data to an RMS of 1.0.

contrary a *resistive* lower crust is very rare. Haak and Hutton (1986) define a lower crust with a resistivity in the range of 100–300 Ω m as *normal*. Precambrian regions have a typical lower crustal conductance (conductivity × thickness) of around 20 S, whereas Phanerozoic regions have a conductance more than an order of magnitude higher, 400 S (Jones, 1992). Accordingly, given the almost ubiquitous existence of conducting zones within the crust, defining the actual resistivity of the mantle beneath the continents is a difficult task that still needs attention.

5. Electrical asthenosphere

From the earliest MT measurements made on the continents, it was recognised that there had to be a region of high conductivity (low resistivity) at some depth in the continental upper mantle to explain the long period descending branch of the apparent resistivity curves. Comparison of the depth to this conducting zone with the depth to the seismic low velocity zone associated with the asthenosphere showed generally good agreement as early as 1963 (Ádám, 1963; Fournier et al., 1963), and studies since have continued to corroborate the correlation (see below). Accordingly, this conducting zone has been termed the *electrical asthenosphere*.

In 1983 an International Union of Geodesy and Geophysics Inter-Association Working Group was established by the International Associations of Seismology and Physics of the Earth's Interior (IASPEI) and Geomagnetism and Aeronomy (IAGA) on Electromagnetic Lithosphere–Asthenosphere Soundings (ELAS) to work with the ELAS group which had been active in IAGA since 1978. Gough (1987) gave an interim report of the activities of the group. A

number of investigations in many countries have been carried out under the auspices of ELAS, with one of the most well-known being the EMSLAB (electromagnetic study of the lithosphere, asthenosphere and beyond) study of the Juan de Fuca subduction zone (Booker and Chave, 1989).

Based on empirical evidence, Ádám (1976) proposed that the depth to the conducting ELAS layer beneath the continents can be predicted from the formula

$$h = 155q^{-1.46}$$

where h is the depth in km, and q is the heat flow in heat flow units. This formula is inappropriate for some regions (such as the Slave craton in northwestern Canada with a measured heat flow of ~ 1.2 HFU at Yellowknife, but no conducting layer at ~ 120 km), but appears to be reasonably valid for others.

Using ocean-bottom instrumentation, MT measurements in the North Pacific revealed the existence of an electrical asthenospheric layer by the early 1970s (reviewed by Filloux, 1973). Measurements have now been made in most of the world's oceans, and this general result has been confirmed. Data from locations of varying lithospheric age in the North Pacific demonstrate that the top to the asthenospheric conductor deepens as the age of the lithosphere increases (Oldenburg et al., 1984; Tarits, 1986). With a mean conductance value of 5000 S, and a thickness of 100 km taken from seismic information, Vanyan (1984) used these North Pacific data to suggest that the typical resistivity of the oceanic asthenosphere is about 20 Ω m.

Fig. 4 shows a comparison of the MT responses expected above a mantle with and without an asthenospheric zone. The two resistivity-depth models are also shown in the figure (on a logarithmic-depth scale). The reference profile has a resistive crust and

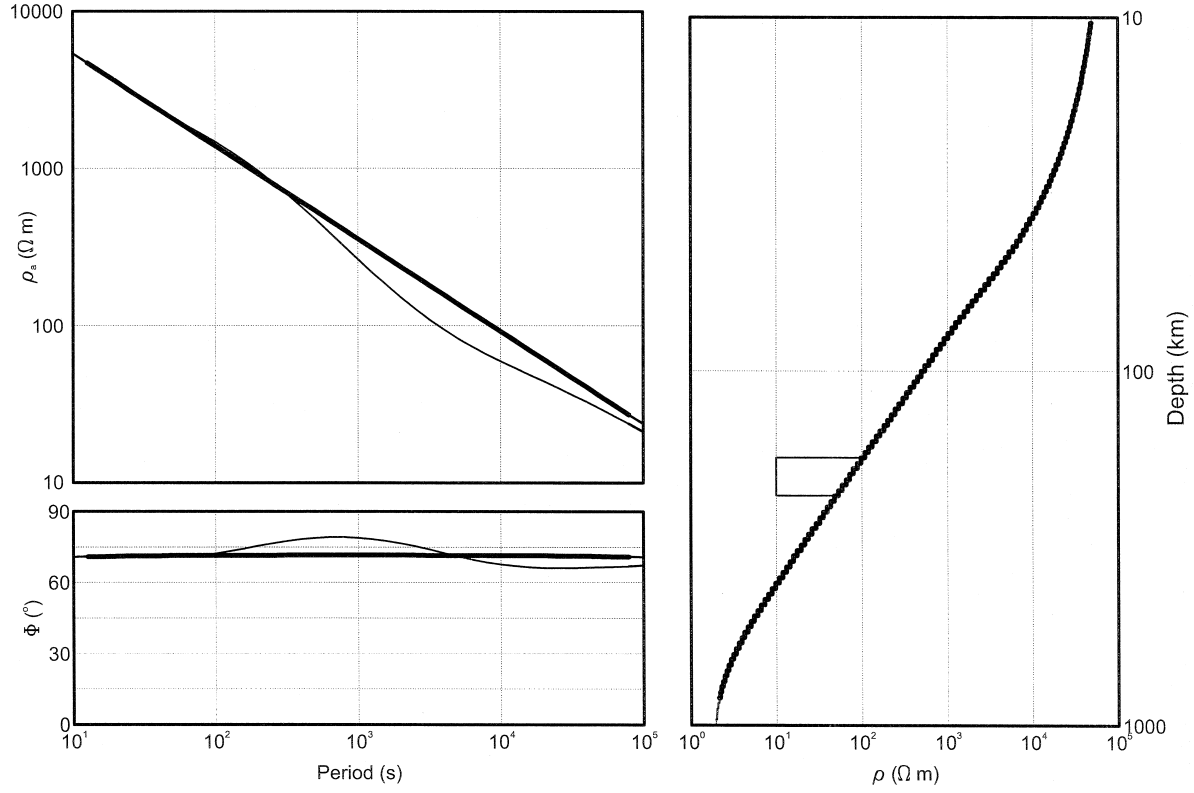

Fig. 4. The responses of the reference model (heavy lines) compared to those from the same model with additionally an asthenospheric zone.

mantle without any conducting zones. It was obtained by inverting the East European Platform response of Vanyan et al. (1977), assuming 10% scatter and error on the theoretical data, using the Occam smooth inversion of Constable et al. (1987). The model with the asthenospheric layer is the same as the reference profile, but with a 50-km-thick zone of 10 Ω m resistivity (total conductance of 5000 S) from 175–225 km depth extent. The difference in total conductance between the reference model and the asthenospheric model is 4200 S. Clearly the difference between these two models would be apparent in all but the poorest MT data. Sensitivity to the existence of the asthenospheric layer is in the period range 1000–30,000 s for the apparent resistivity data, with the maximum difference at around 5000 s (where the asthenospheric model phase crosses the reference model phase), with 150 Ω m for the reference model compared to 32 Ω m for the asthenospheric model.

Commonly, however, there exist conducting zones within the crust which can have the effect of shielding this asthenospheric response. Fig. 5 shows the response for a reference model containing a lower crustal conductor (LCC) of 10 Ω m from 20–40 km depth, for a total of 2000 S conductance, compared to a model including an asthenosphere. The effect of the asthenospheric zone is now more difficult to detect and is at longer periods. At 10,000 s, the difference between the two apparent resistivity data is a factor of three, with 61 Ω m without an asthenosphere compared to 21 Ω m with one, which is over half-an-order of magnitude and should be easily resolvable in high quality data. However, the difficulty resolving the asthenospheric zone occurs because the conductance within the zone can be smeared out over a greater depth range. Synthetic data, with 10% error and scatter in apparent resistivity and equivalent in phase (2.9°), generated from the model containing both a conducting lower crust and as-

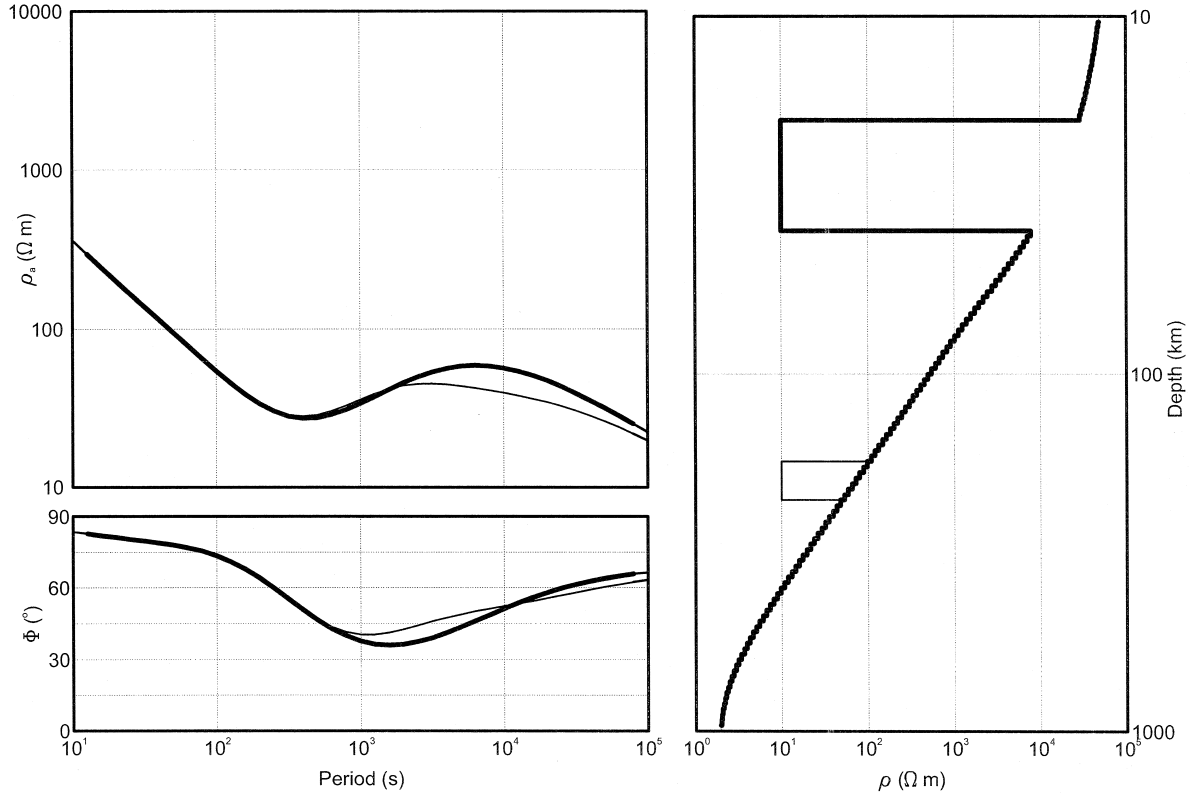

Fig. 5. The responses of the reference model with a lower crustal conductor (heavy lines) compared to those from the same model with additionally an asthenospheric zone.

thenosphere, when inverted using Occam to find the smoothest model fitting the data to a normalized RMS of 1, yields a model without a readily identifiable low resistivity zone representing the asthenosphere (Fig. 6).

This screening problem becomes exacerbated if other conducting zones exist within the lithosphere, such as a surficial sedimentary basin or mid-crustal fault zones. As a general rule-of-thumb, we cannot usually sense the existence of an anomalous region if its conductance is less than the total conductance from the surface down to that depth.

There appears to be a correlation in the literature between the existence and conductance of electrical asthenospheric zone, and the existence and conductance of a lower crustal conductor. This may be an artifact of the screening effect of the LCC discussed above, and there may not be a tectonic or geodynamic reason for such a correlation. However, in some situations there may be a causative relationship, such as a thin lithosphere with a correspondingly shallow asthenosphere leading to a partially-molten, wet lower crust, such as the southern Canadian Cordillera (Jones and Gough, 1995).

Selected observations of the electrical asthenosphere are summarized in Table 1, and Praus et al. (1990) gives a comprehensive table of observations in central Europe to 1990. Estimates of the resistivity of the electrical asthenosphere are usually around 5–20 Ω m. Commonly, this ELAS layer is interpreted as a region of partial melt, given its correlation with the seismically-defined asthenosphere. For a host resistivity of 1000 Ω m, and a melt resistivity of 0.1 Ω m, a melt fraction of 1–3% is sufficient to explain this resistivity for most pore geometries. Partial melt should be gravitationally stable below

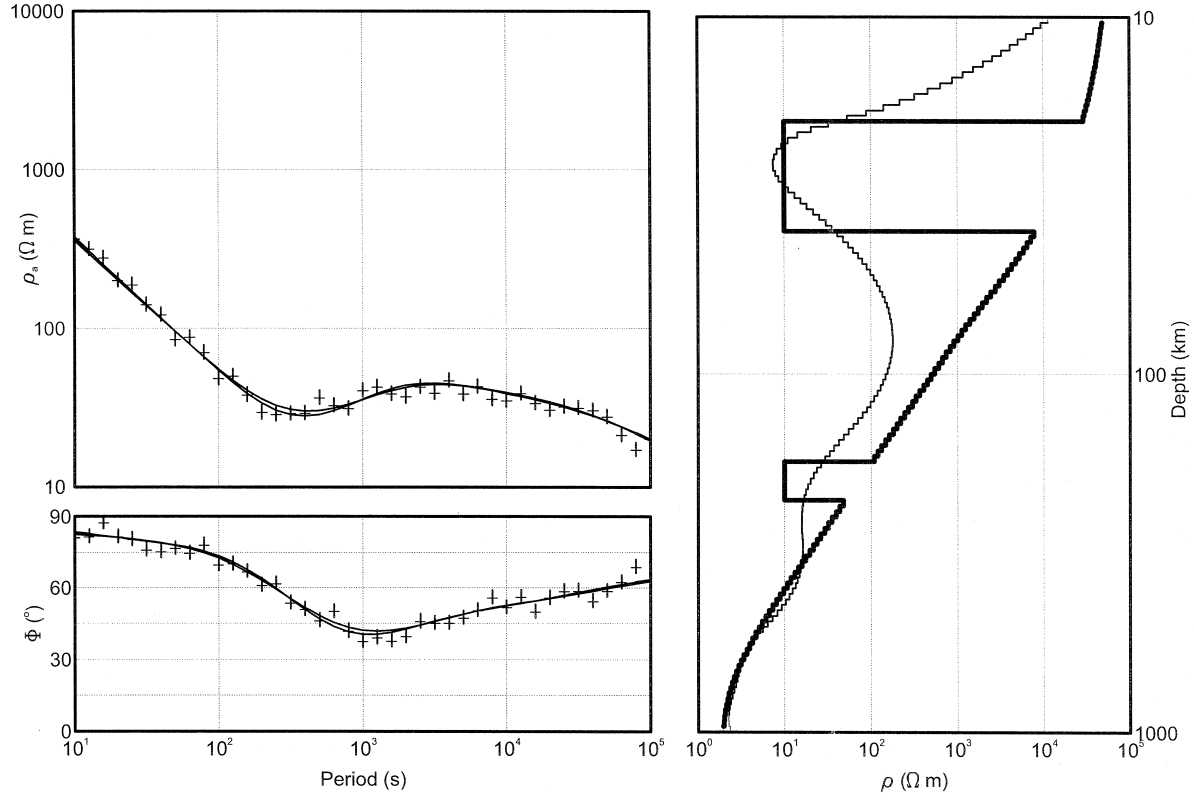

Fig. 6. Synthetic data (with 10% scatter and error) generated from the reference model with a lower crustal conductor and an asthenospheric zone (heavy lines). The smooth model fits the synthetic data to an RMS of 1.0. The response of the two models are the same to within data error.

Table 1
Global observations of the electrical asthenosphere

Region	Depth (km)	Resistivity (Ω m)	Reference and Comments
Eastern USSR			
Kamchatka peninsula	80–>100	10–20	(Moroz, 1985, 1988) Doming of asth. below centre of peninsula corr. with crustal cond. layer and heat flow maximum
Sakhalin island	70–>120+	5–10	(Kosygin et al., 1981) Doming of asth. below island corr. with crustal cond. layer. (Vanyan et al., 1983) No asth. below continent. Sakhalin has low heat flow(1 HFU)
Turanian Shield	80–120		(Kharin, 1982 reported in Roberts, 1983)
Siberian Shield	100		(Safonov et al., 1976; Pavlenkova and Yegorkin, 1983) Corr. with zone of lesser heterogeneity
Nizhnyaya Tunguska river	50–>100		(Safonov et al., 1976) dipping from West–East
Baikal	15–>25	20	(Berdichevsky et al., 1980)
Eastern Europe			
Pannonian Basin	50–>80		(Ádám et al., 1983) corr. with LVL at 57–>75 km
Central Europe			
Rhenish Shield	100–>150	10	(Bahr, 1985) seismics gives 100 km
Northern Europe			
Northern Sweden	157–190	2.5–8	(Jones, 1980, 1982, 1984; Calcagnile, 1982, 1991; Jones et al., 1983; Calcagnile and Panza, 1987), corr. with sesimic asth.
Kola peninsula	105	80	(Vladimirov, 1976) data could not resolve actual resistivity of the layer (Krasnobayeva et al., 1981)
West Spitzbergen	115	1	Oelsner (1965)
Karelian megablock			
West Africa			
Senegal	300–>500	10	(Ritz, 1984) shallower under Phanerozoic than under Precambrian
Australia			
Central Australia	200	10	(Lilley et al., 1981) band-limited data of very poor quality
Eastern Australia	60–150	1	(Spence and Finlayson, 1983)
	90	20	Whiteley and Pollard (1971) asth. not resovable with these data
	70–150	2–60	Moore et al. (1977) asth. barely resolvable with these data

200 km (Agee and Walker, 1993). Lizarralde et al. (1995) offer an alternative hypothesis for the ELAS layer when it is shallower than 200 km, and that is the presence of water, which enhances conductivity by H^+ ionic conduction (Karato, 1990), dissolved in a depleted, anisotropic, olivine mantle. Free water should not exist in the mantle except at unique tectonic environments, such as in the mantle wedge above a subduction zone (Kohlstedt et al., 1996).

Why should the electrical asthenosphere layer be bounded? The MT observations suggest that the electrical asthenosphere layer is of finite thickness extent. Once partial melt starts, why should it cease at greater depths? Perhaps the answer lies in the shape of the solidus for the mantle mineral and the geometry of the geotherm.

Figs. 7 and 8 show the solidus for a peridotite that is ''wet'', 0.3 wt.% H_2O and 0.7 wt.% CO_2 (Fig. 7a and Fig. 8a) compared to ''dry'', <0.004 wt.% H_2O (Fig. 7b and Fig. 8b) (Olafsson and Eggler, 1983). On Fig. 7a,b are also shown the continental geotherm of Sclater et al. (1980) and on Fig. 8a,b that of Tozer (1972, 1979). Note that neither geotherm will explain the existence of an electrical asthenosphere layer for a dry peridotite, but both cross the solidus for a wet peridotite. However, Sclater's geotherm suggests that the electrical asthenosphere layer should be of infinite extent,

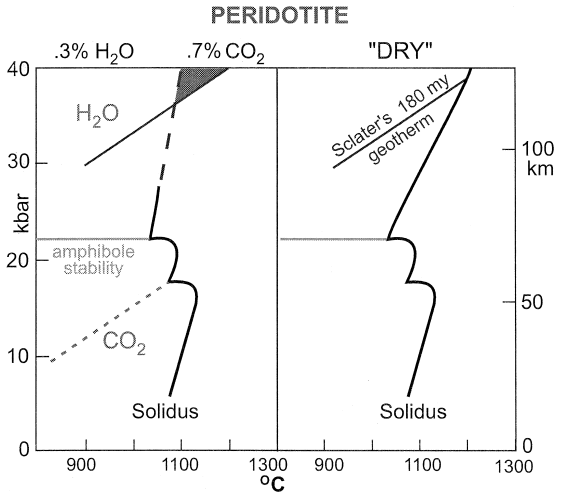

Fig. 7. Peridotite solidus for (a) ''wet'' (0.3 wt.% H_2O, 0.7 wt.% CO_2) and (b) ''dry'' (<0.004 wt.% H_2O) conditions (from Olafsson and Eggler, 1983) compared to the geotherm of Sclater et al. (1980). Note that the geotherm crosses the wet solidus at approx. 35 kbar and does not recross it.

whereas Tozer's geotherm recrosses the solidus to give a layer of limited extent.

6. Deep mantle observations

Imaging the deep mantle conductivity with reasonable resolution is in its infancy compared to seismological studies. Although there is now compelling seismological evidence for a sharp boundary at the 410 km discontinuity (Vidale et al., 1995), the evidence from EM studies has been equivocal. Indeed, as pointed out by Campbell (1987), models derived from global or large-scale regional EM studies prior to about 1969 usually included an increase in conductivity at 400 km depth, whereas later studies generally did not.

Two problems make resolving the mantle resistivity at depths of some hundreds of kilometres difficult. The first is the screening effect of the asthenosphere layer, and the second is due to the natural magnetic field spectrum. Electromagnetic waves are attenuated more strongly in conducting layers than resistive ones, and so one must go to longer and longer periods in order to penetrate through a conducting region. This is not a problem in the crust or uppermost mantle, as the external natural source magnetic fields increase in power with increasing period. However, at periods beyond those that sense the asthenosphere, or around 10,000 s, the power spectrum shows a rapid decrease, with spectral lines at the harmonics of the daily variation (24 h, 12 h, 8 h, 6 h and 4 h are useful). In addition, for a uniform Earth and for the same driving magnetic field power, the electric field decreases in strength with increasing period. This decrease is exacerbated as electrical conductivity decreases with period, i.e., increasing depth, in the Earth.

There have been a number of attempts to obtain the Earth's deep conductivity. Most of these using either (i) spherical harmonic analysis of the global observatory observations (e.g., Banks, 1969), (ii) the geomagnetically quiet day source field structure (*Sq*, e.g., Schmucker, 1985; Olsen, 1998) or (iii) long electric dipoles at geomagnetic observatories (e.g., Egbert and Booker, 1992, using Tucson observatory). The response functions from these studies are generally quite poor in that their errors are typically greater than 10%. Also, the one-dimensional (1D) assumption inherent in the application of methods (i) and (ii), and usually adopted in the interpretation of method (iii), is hardly ever shown to be valid.

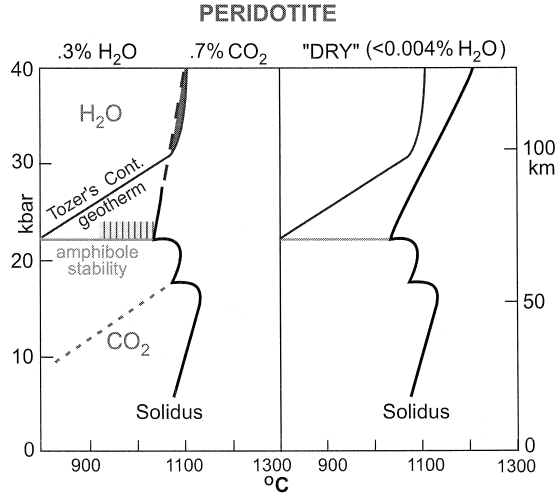

Fig. 8. Peridotite solidus for (a) ''wet'' (0.3 wt.% H_2O, 0.7 wt.% CO_2) and (b) ''dry'' (<0.004 wt.% H_2O) conditions (from Olafsson and Eggler, 1983) compared to the continental geotherm of Tozer (1972, 1979). Note that the geotherm crosses the wet solidus at about 30 kbar and then recrosses it at about 40 kbar. The dry solidus is not crossed by the geotherm.

A novel experiment undertaken by Schultz et al. (1993) in a lake in central Ontario, Canada, obtained high quality long period response function estimates by using long electrode lines (1 km) with the electrodes in a chemically- and thermally-stable environment (bottom of the lake). Recordings of the time-varying five-component electromagnetic field were made for over 2 years at the Carty Lake site, and at a second site some 30 km distant the three-component magnetic fields were recorded to use as a ''remote reference'', familiar in economic theory since the early 1940s (Reiersol, 1950), to remove bias in response function estimation (see, e.g., Gamble et al., 1979). The site was chosen because of its location in the centre of a large Archean craton (Superior province) and from the observed crustal regional electrical homogeneity (Kurtz et al., 1993). The data from the lake site fill the gap between conventional land-based MT responses (to 2 h) and the long period observatory responses (from 6 days). This range was demonstrated to be critical for resolving a peak in conductivity centred at around 450 km (Fig. 9) with a resolving kernel of about 100 km width. Without these lake bottom responses, the peak at 450 km disappears and there is no resolution of the decrease in conductivity below that depth. Using a genetic algorithm approach, Schultz et al. (1993) searched the model space of an overparametrized Earth, and were unable to find acceptable models that excluded an abrupt increase in conductivity near 230, 425 and 660 km, and at these depths conductivity must rise above 0.02 S/m (below 50 Ω m resistivity), 0.06 S/m (16.7 Ω m) and 0.3 S/m (3.3 Ω m), respectively.

For western North America, Egbert and Booker (1992) find that a step increase in conductivity at around 400 km is consistent with, but not required by, the estimated responses (Fig. 9; dashed line). A resolvable peak in conductivity at around the 410 km seismic discontinuity is not found in mantle conductivity models from western Europe (e.g., Bahr et al., 1997; Olsen, 1998) although the non-1D aspects of the data suggest that a 1D interpretation may be invalid. Note that the two models for North America, one for the Superior craton and the other for western North America, suggest that the two regions have different physical properties to about 600 km depth. This implies that the craton does indeed have a deep

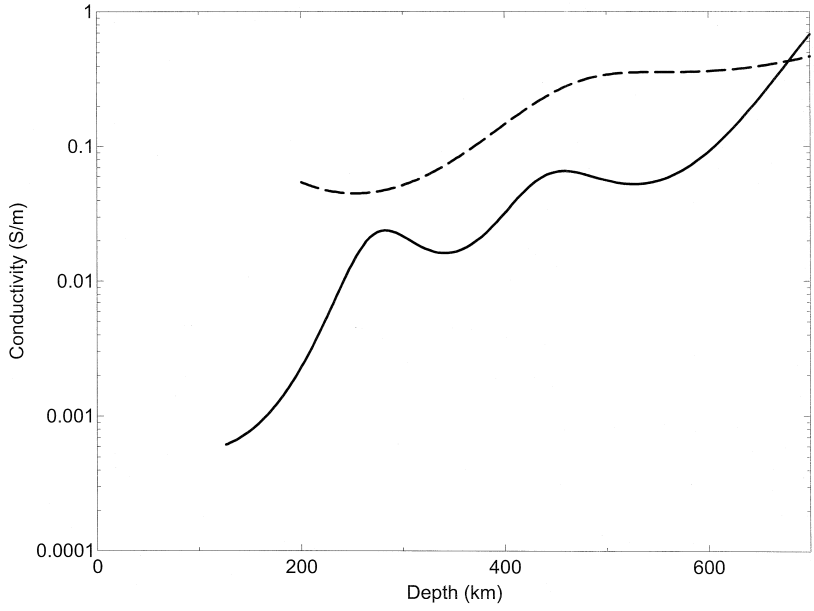

Fig. 9. Smooth inversion of the data from the Superior craton (solid line) and from western North America (dashed line). Note the peak in conductivity at around 450 km for the Superior craton, and the rise in conductivity at 400 km for the western North American model (from Schultz et al., 1993 and Egbert and Booker, 1992, respectively).

root that may extend beyond the 410 km discontinuity.

Recent laboratory experiments present evidence for a step increase in two orders of magnitude in electrical conductivity at the 410 km discontinuity as a consequence of the phase change of olivine to higher pressure mineralogy (wadsleyite) (Xu et al., 1998). A large step increase cannot be resolved using surface data if one obtains a conductivity model with least structure, such as Occam (Constable et al., 1987), even for highly precise data (1% error as shown in Fig. 10b, dotted line). However, with a priori knowledge of the likelihood of a step increase, one can re-perform the inversion without a smoothness penalty at that boundary. The resulting models, for 10% (Fig. 10a) and 1% (Fig. 10b) error data, are consistent with the responses and include the step discontinuity. Note that the models from the responses with higher error are more oscillatory due to a Gibbs-like phenomenon, whereas the step-model for 1% error is almost exact (dashed line, Fig. 10b).

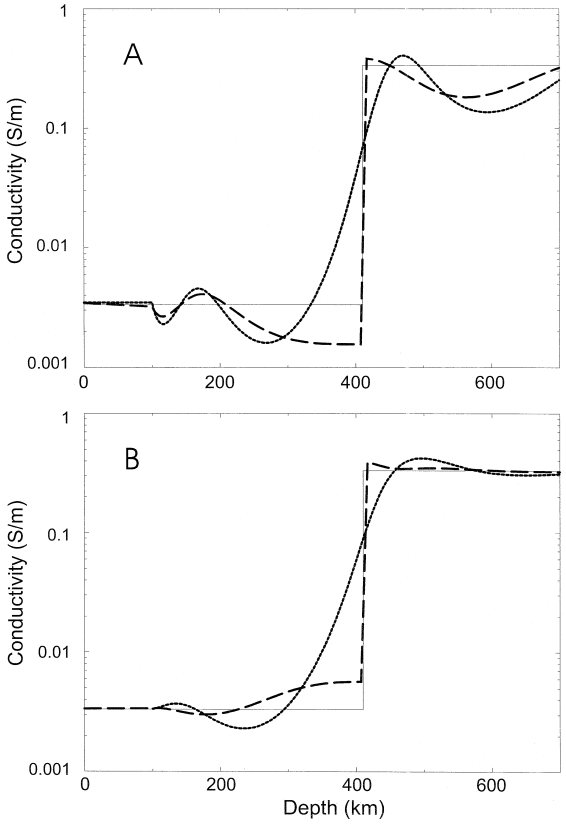

Fig. 10. Smooth models derived from synthetic data generated from a model with a step transition at 410 km from 0.00333 S/m (300 Ω.m) to 0.333 S/m (3 Ω m) (thin line) for (a) 10% error in impedance, and (b) 1% error in impedance. Dotted lines are for models without any discontinuity, whereas the dashed lines are for models with an unpenalised discontinuity at 410 km.

With knowledge of this sharp increase in conductivity due to olivine phase change, new high quality data need to be acquired in appropriate regions to test whether the mantle can be effectively described by an olivine mineralogy, or whether the role of volatiles must be invoked. One observation that requires explanation is the observation by Schultz et al. (1993) that mantle conductivity decreases below about 450 km, whereas a phase change from wadsleyite to ringwoodite at 510 km should result in a minor increase in conductivity (Xu et al., 1998).

7. Mantle electrical anisotropy

Whereas there has been an explosive growth in the number of observations of seismic SKS shear wave splitting, interpreted as indicative of seismic anisotropy in the lithospheric mantle, there have been very few comparable interpretations of electrical anisotropy. In the main, this has been because the MT community has focused more on using the method to solve crustal-scale problems over the last decade. However, there can also be an ambiguity in the interpretation of MT data in terms of whether the difference between the two modes of propagation is due to 2D *structure*, or whether it must be attributed to 2D *anisotropy* on a scale smaller than the resolving power of the technique. For example, the two models in Fig. 11 — model A with a lower crustal fault juxtaposing two regions of very different resistivity and model B with a host of 2000 Ω m cross-cut by conducting dykes of 5 Ω m — give the same MT response at the observation site (Cull, 1985). The difference between them is in the vertical magnetic field response. Model A will have a large H_z response due to the fault, whereas model B will have virtually no measurable H_z.

So far there has only been one convincing example of a very strong difference in MT response in the

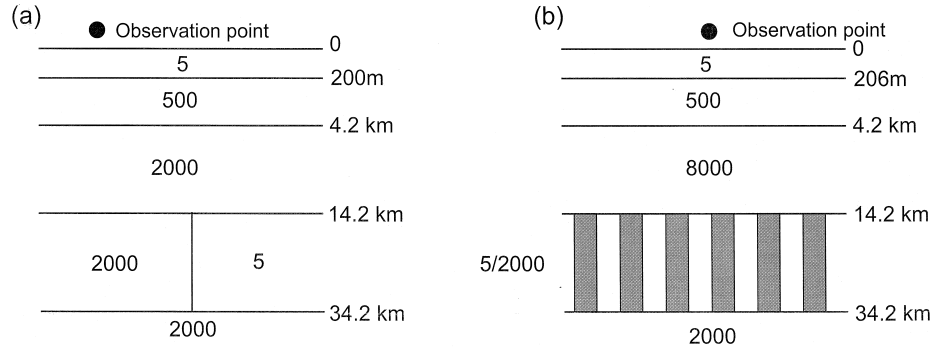

Fig. 11. Two models of the lower crust which fit MT observations in Australia. Model A is of a faulted contact in the lower crust, whereas model B is of numerous repetitive resistive dykes (2000 Ω m) cutting a conducting (5 Ω m) lower crust (redrawn from Cull, 1985).

two orthogonal directions without any vertical field response observed, and that is the work of Mareschal et al. (1995) in the Superior Province of Canada. Subsequent SKS work in one region (across the Grenville Front) by Senechal et al. (1996) showed that the fast seismic direction is almost parallel to the high conductivity direction, but there is a small but statistically-meaningful obliquity between them. This obliquity has been interpreted by Ji et al. (1996) as an indicator of the movement sense on ductile mantle shear zones. Support for this hypothesis comes from a recent MT survey across the Great Slave Lake Shear Zone (GSLsz) which yielded anisotropic data at periods sampling upper mantle depths (50 km) with the direction of maximum conductivity at N35E, which is oblique to the strike of the GSLsz of N45E (Jones et al., 1997). The corresponding SKS measurements have yet to be undertaken.

8. Laboratory conductivity studies on mantle rocks

An informative example of the role of a minor conducting phase is the two-phase mixture H_2O ice–KCl aqueous solution as an analogue for partially molten Earth materials (Watanabe and Kurita, 1993). This system has well-defined phase diagrams and equilibrium structures. When the KCl concentration is lower than the eutectic concentration (19.7 wt.% at atmospheric pressure), H_2O ice and KCl aqueous solution coexist at a temperature between the liquidus and the solidus. It also represents a strong contrast in resistivity between solid and melt phases. The variation in conductivity with temperature for 0.2 wt.%, 0.4 wt.% and 0.6 wt.% KCl is shown in Fig. 12. A dramatic increase in conductivity at the solidus is followed by an increase that can be described by Archie's Law (power exponent of 1.34 to 1.74) to the liquidus. This shows that even at very low melt fractions, much less than 1% melt, the KCl solution is well interconnected, approaching a connectivity of unity. The conduction process goes from (A) inefficient electronic conduction through the solid ice to (B) efficient ionic conduction in the melt phase at the solidus, to (C) more efficient ionic conduction as the melt fraction rises dramatically at the liquidus (Fig. 13), to (D) completely efficient ionic conduction in the totally liquid phase. Comparisons of the effect of partial melting on physical parameters for this system demonstrate that a melt fraction less than 5% causes electrical conductivity to increase by 1.5–3 orders of magnitude (Fig. 12), whereas the seismic velocity decreases by only a few percent (Watanabe and Kurita, 1994).

Laboratory studies on candidate samples of the continental upper mantle have been undertaken for over two decades. Most of the work has concentrated on single crystals of olivine, although some studies have been undertaken on polycrystalline compacts. Reports from different laboratories on various samples were initially very disparate until the role of oxygen fugacity was understood (Duba, 1976), but recent work shows much better agreement (Fig. 14, from Constable et al., 1992). A parametric model

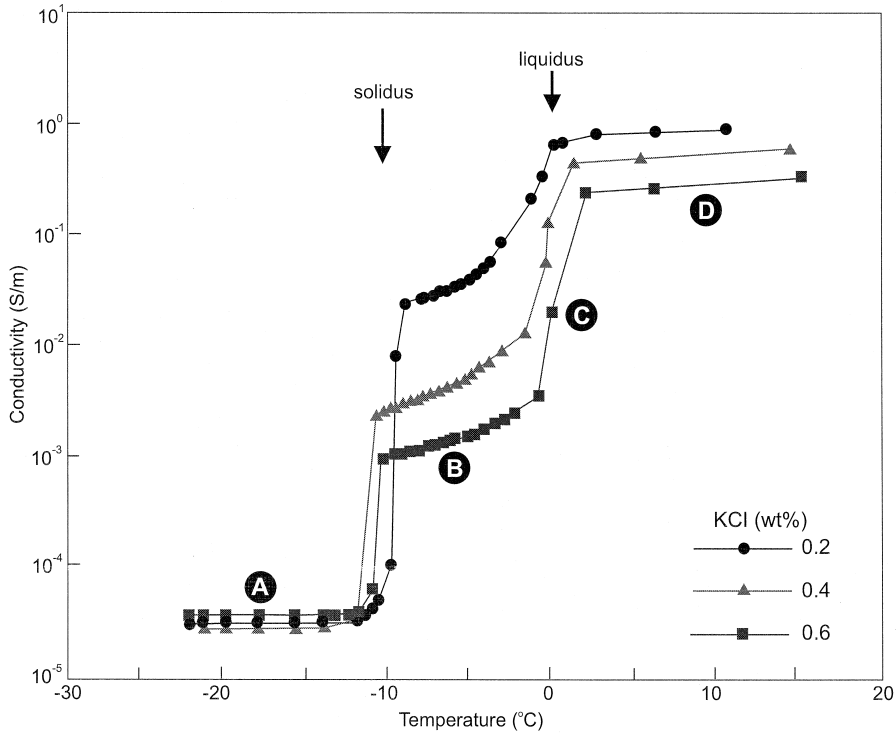

Fig. 12. Conductivity variation with temperature of the two-phase mixture H_2O ice–KCl with differing weight percent KCl (redrawn from Watanabe and Kurita, 1993). There are four conduction regions. Region A is where there is inefficient electron conduction through the solid ice. Region B and C describe efficient ionic conduction in the melt phase. Region D is completely saturated ionic conduction in the totally liquid phase.

description of the studies is, to a reasonable approximation,

$$\sigma = 10^{2.402} e^{-1.60\,eV/kT} + 10^{9.17} e^{-4.25\,eV/kT}$$

in the temperature range 720°C–1500°C (Constable et al., 1992). The conduction mechanism is predominantly by electron holes at low temperatures, but then is superseded by magnesium vacancies at high temperatures (Schock et al., 1989).

This equation predicts that for a pure olivine mantle, the resistivity at 750°C should be of the order 300,000 Ω m, which is far higher than observed under the one region where we have an excellent estimate of the mantle resistivity due to the lack of any crustal conductors, the Slave craton, and crustal resistivity is in excess of 40,000 Ω m (Jones et al., 1997). The uppermost upper mantle has a resistivity around 4000 Ω m, which would imply a temperature of almost 1100°C — which is clearly unreasonable. Accordingly, the upper mantle beneath the Slave craton cannot be pure olivine, and there must be other constituents in the rock matrix creating conducting pathways.

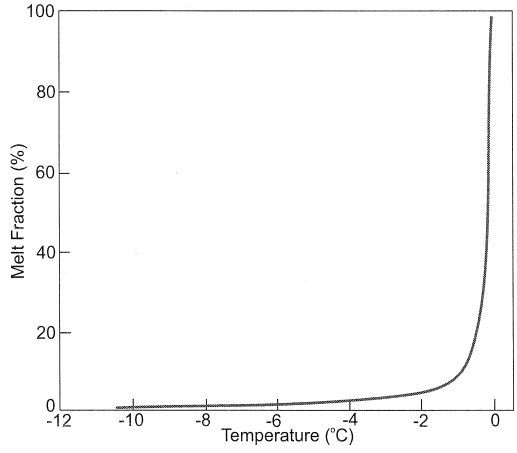

Fig. 13. Variation of melt fraction with increasing temperature in the two-phase mixture H_2O ice–KCl (redrawn from Watanabe and Kurita, 1993).

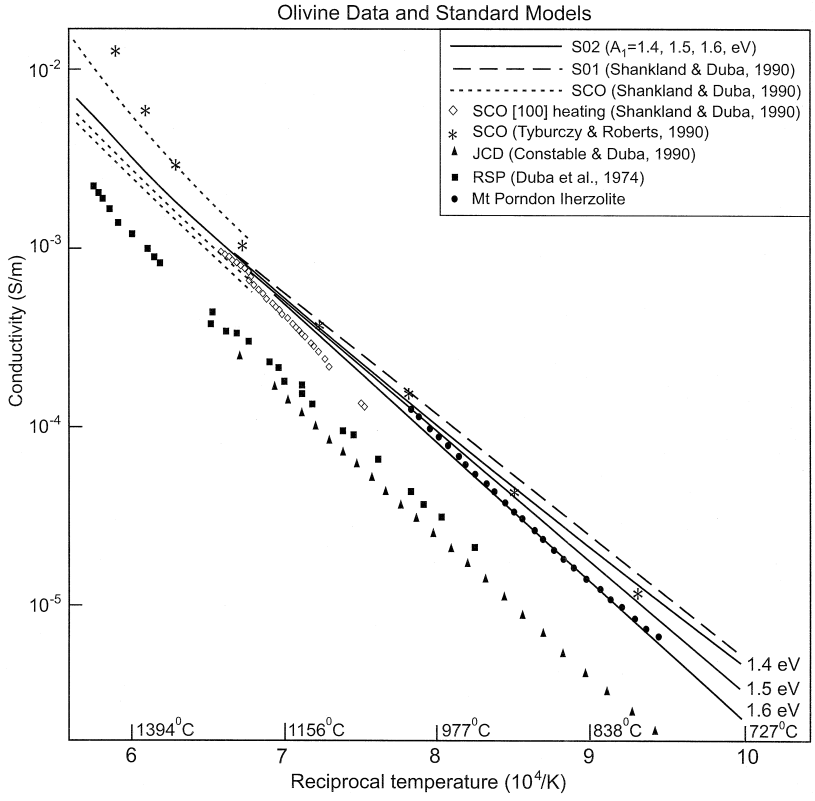

Fig. 14. Comparison of olivine laboratory temperature–conductivity data and standard models (Constable and Duba, 1990; Duba et al., 1974; Shankland and Duba, 1990; Tyburczy and Roberts, 1990) (redrawn from Constable et al., 1992).

Laboratory studies of partially molten gabbro by Sato and Ida (1984) and Sato et al. (1986) demonstrate that the volume percent of connected melt increased dramatically in the temperature range of 1127°C to 1200°C from undetectable to 17%. Recent work by Tyburczy and Roberts (1990) shows that melt composition is important for melt conductivity.

For the deep mantle, as reported above recent work by Xu et al. (1998) demonstrate that there should be a rapid increase in electrical conductivity at the 410 km boundary as olivine undergoes a phase change to wadsleyite. At 520 km there is a minor increase as wadsleyite transforms to ringwoodite.

9. Correlation of electrical and seismic asthenospheres

The existence of a conductive layer within the mantle at the same depth as the low velocity layer corresponding to the asthenosphere was proposed 35 years ago independently by Ádám (1963) and Fournier et al. (1963). Laboratory studies demonstrate that partial melt will have an effect on both seismic velocities and electrical conductivity (Schmeling, 1985, 1986; Watanabe and Kurita, 1994).

An early comparison of asthenospheric zones for the Soviet Union, defined by regions of low velocity and regions of high conductance, shows good spatial correlation (Fig. 15, redrawn from Alekseyev et al., 1977). There has not been a systematic and critical global comparison undertaken to date, but collocated studies demonstrate that this correlation may be common. Calcagnile and Panza (1987) discuss the correlation of results obtained by inversion of surface-wave dispersion data and P-wave travel time observations with those obtained by EM studies for Europe. Praus et al. (1990) compiled data on the MT and seismic determination of the depth to the as-

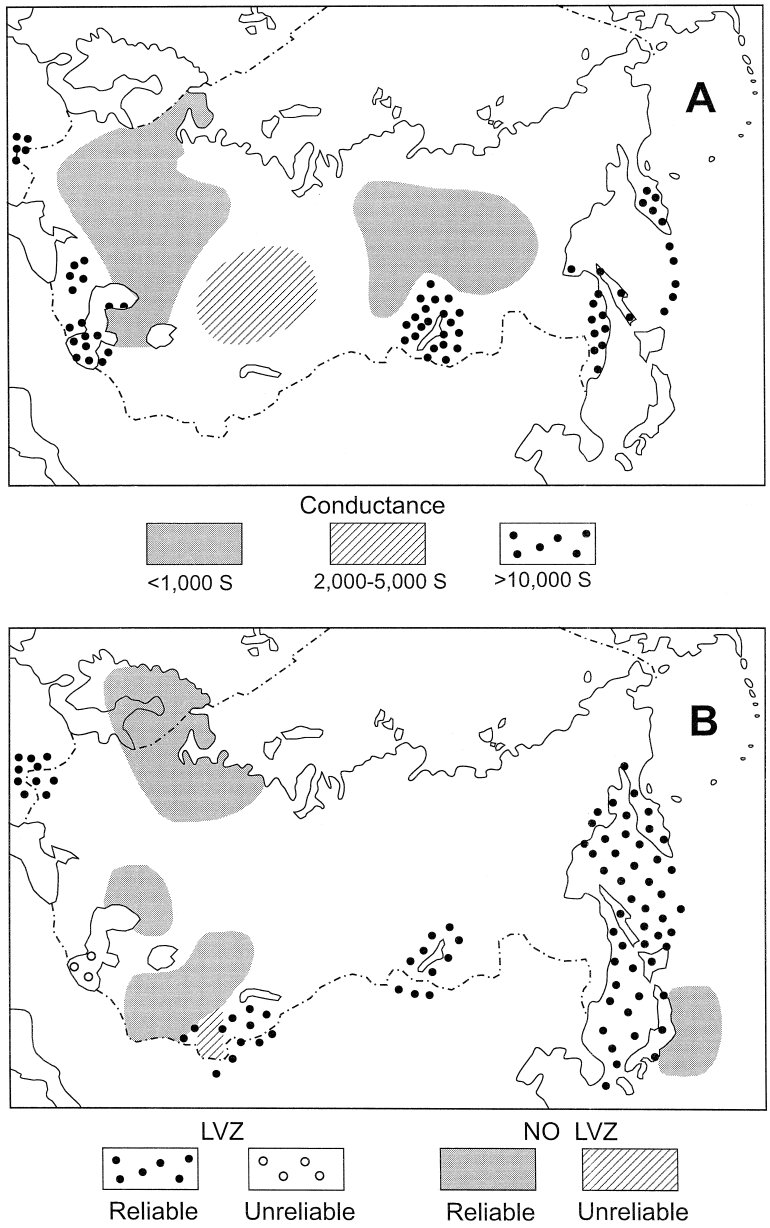

Fig. 15. Comparison of regions of high conductance (A) and low velocity zones (B) (redrawn from Alekseyev et al., 1977).

thenosphere in central Europe, and found good correspondence between the two datasets.

One cratonic region where there is good correspondence between the base of the lithosphere defined electrically and seismically is the Baltic shield. Early work by Calcagnile (1982), using Rayleigh-wave dispersion data, gave lithospheric thickness variation over Fennoscandia shown in Fig. 16a. More recent analysis by Calcagnile (1991), using higher modes, gave a shear wave velocity-depth profile for the path from Copenhagen to Kevo (COP to KEV on Fig. 16a) which exhibits a low velocity zone starting at a depth of around 210 ± 30 km and is 20–80 km in thickness extent (Fig. 16b). This model crosses a

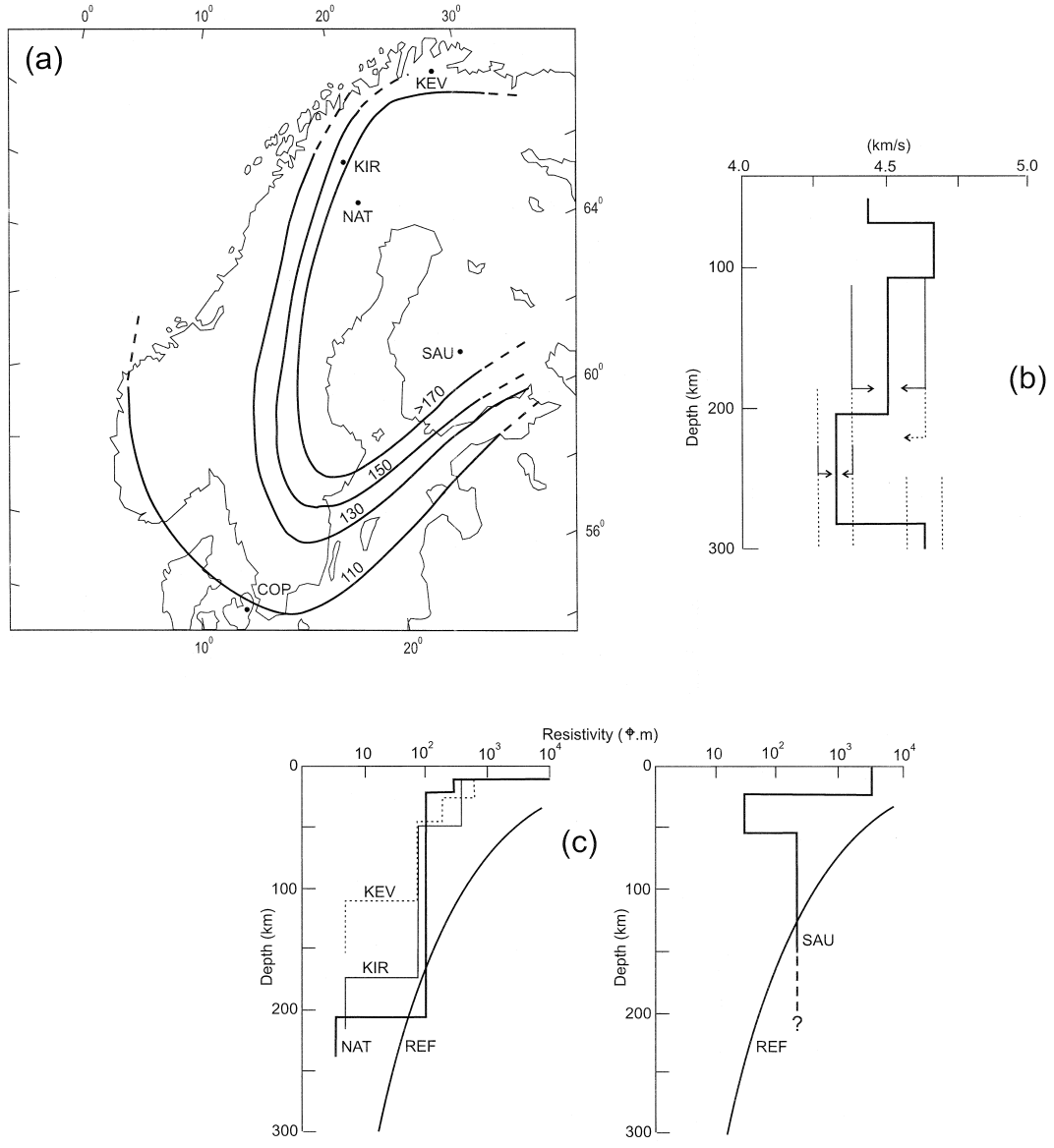

Fig. 16. a) Lithospheric thickness map for Fennoscandia defined by Calcagnile (1982). (b) Shear wave velocity model for the path COP-KEV (Calcagnile, 1991). (c) Resistivity models for regions of the Baltic shield defined by Jones (1980, 1982, 1984) and Jones et al. (1983).

range of lithospheric thicknesses in the map of Fig. 16a, and is considered by Calcagnile (1991) to represent the average model for the Baltic shield. Resistivity-depth models derived from EM experiments for four regions of the Baltic shield are shown in Fig. 16c, together with the ''reference'' model discussed above (REF in Fig. 16c). Models for Kiruna (KIR) and Nattavaara (NAT) were obtained using two different EM methods and using different magnetic source field morphologies. For KIR (and KEV) the horizontal spatial gradient (HSG) approach was used (Jones, 1980, 1982, 1984) on only winter-time high-activity magnetic field time series, whereas for NAT (and SAU) the magnetotelluric method was applied to summer-time low-activity electric and magnetic time series (Jones et al., 1983). Although the HSG

results have been questioned due to the possible effects of highly non-uniform source fields (Osipova et al., 1989), event-averaging and the analysis approach applied to the HSG data should have mitigated these problems. Also, the correlation of the KIR and NAT models, given the different approaches and disparate datasets, lends credence to their veracity. The published model for NAT was obtained using a Monte-Carlo search approach (Jones and Hutton, 1979b), and gave a lithospheric thickness of $211 + 14/-10$ km (Jones et al., 1983). Inverting the NAT data using a modern layered inverse method, the best model has a lithospheric thickness of 213 km with a standard error of $+26/-23$ km.

Accordingly, the average depth to the base of the seismologically-defined Baltic shield lithosphere is 210 ± 30 km, and the depth to the base of the electrically-defined lithosphere beneath NAT is 213 $\pm$ 24 km. Whilst this remarkable correspondence of the means is far superior than their stated errors, it is clear that there is a statistical correlation between the two. Also, the thinning of the lithosphere to the edges of the Baltic shield, imaged seismically in the map of Fig. 16a, is in agreement with the shallowing of the depth to the electrical asthenosphere beneath KIR and KEV and with the lack of detection of an asthenosphere beneath SAU shallower than about 150 km. (Penetration at SAU is poor because of the lower crustal conducting zone, and also because the response was not defined to sufficiently long periods.) MT measurements at 31 locations in central Finland around SAU show that there is no well-developed asthenosphere, i.e., with conductance greater than 500 S, to 300 km (Korja, 1993).

10. Conclusions

Natural-source EM studies of the continents have contributed to our knowledge of their cratonic roots by:

1. Defining the base of the resistive cratonic lithosphere.
2. Imaging the electrical asthenosphere and showing that it correlates with the seismic upper mantle low velocity zone.
3. Demonstrating that there must be some conducting component within the olivine/peridotite matrix that is not present in oceanic mantle lithosphere.
4. Inferring that the continental geotherm must cross the solidus twice to explain the limited depth extent of the electrical asthenosphere layer.

Comparisons of the lithospheric thickness derived seismologically and electromagnetically appear to show good correspondence. Thus, there are likely to be significant advances in our understanding when collocated deep seismic and EM experiments are performed, and their datasets jointly inverted.

There are many more contributions to be made by deep EM studies. For example, Tozer (1979, 1981) argues that, at the microscopic level, conductivity may be closely related to viscosity. This is highly significant when considering lithospheric processes: conductivity anomalies may be interpreted not only in terms of heat flow anomalies but as zones of possible convection and other transport phenomena. Geometries of the lithosphere–asthenosphere boundary can be imaged to provide data for geodynamic models such as those of De Smet et al. (1998, this issue). Also, hypotheses regarding the lithospheric mantle creation and development, outlined in the Introduction, can be tested using MT data:

Hypothesis 1	The cratonic lithosphere is Archean in age and has been strongly coupled to its crust since that time.
Test 1	The electrical anisotropy must extend smoothly through the cratonic root and be approximately aligned with surface structures. A more exacting test would require that the obliquity between the seismic and EM anisotropy directions must define the same sense of movement as surface structures (Ji et al., 1996 hypothesis).
Hypothesis 2	The cratonic lithosphere is comprised of imbricate stacks formed in the Archean (Helmstaedt and Schulze, 1989 model, with Kusky, 1993 modification).
Test 2	There will be a regional variation in electrical anisotropy direction and possibly in electrical parame-

ters like conductivity or root thickness.

Hypothesis 3 The lithosphere has been added to the craton since the end of the Archean by basal accretion (Thompson et al., 1996 model).

Test 3 There will be no anisotropy and no regional variation in electrical parameters. If either consistent anisotropy or regional variation are observed, then the hypothesis can be rejected.

Hypothesis 4 The old mantle root is of limited spatial extent and its apparent seismically-determined size is caused by transient cold downwelling (Polet and Anderson, 1995 model).

Test 4 There will be no consistent anisotropy direction, no deep anisotropy, and probably a weak electrical signature over most of the craton. The presence of deep anisotropy and an extensive low conductivity root is cause to reject this hypothesis.

Acknowledgements

The author wishes to thank the organizers of the Continental Roots workshop for the opportunity to present this material. Discussions with Alan Chave, particularly regarding the hypotheses and tests in the Section 10, and a critical review from him, greatly improved the submitted version. Reviews by Simon Hanmer and Juanjo Ledo, as well as the editorial remarks by Rob van der Hilst, also contributed to the improvements. Geological Survey of Canada Contribution No. 1998257.

References

Ádám, A., 1963. Study of the electrical conductivity of the Earth's crust and upper mantle. Methodology and results. Dissertation. Sopron, Hungary.

Ádám, A., 1976. Quantitative connections between regional heat flow and the depth of conductive layers in the earth's crust and upper mantle. Acta Geodeat. Geophys. et Montanist. Acad. Sci. Hung. 11, 503–509.

Ádám, A., Vanyan, L.L., Varlamov, D.A., Yegorov, I.V., Shilovski, A.P., Shilovski, P.P., 1983. Depth of crustal conducting layer and asthenosphere in the Pannonian basin determined by magnetotellurics. Phys. Earth Planet Inter. 28, 251–260.

Agee, C.B., Walker, D., 1993. Olivine floatation in mantle melt. Earth Planet. Sci. Lett. 114, 315–324.

Alekseyev, A.S., Vanyan, L.L., Berdichevsky, M.N., Nikolayev, A.V., Okulessky, B.A., Ryaboy, V.Z., 1977. Map of asthenospheric zones of the Soviet Union. Doklady Akademii Nauk SSSR 234, 22–24.

Ashwal, L.D., Burke, K., 1989. African lithospheric structure, volcanism, and topography. Earth Planet. Sci. Lett. 96, 8–14.

Bahr, K., 1985. Magnetotellurische Messung des Elektrischen Widerstandes der Erdkruste und des Oberen Mantels in Gebieten mit Lokalen und Regionalen Leitfahigkeitsanomalien. PhD thesis, Univ. Göttingen.

Bahr, K., 1997. Electrical anisotropy and conductivity distribution functions of fractal random networks and of the crust: the scale effect of connectivity. Geophys. J. Int. 130, 649–660.

Bailey, R.C., 1970. Inversion of the geomagnetic induction problem. Proc. R. Soc. Lond., Ser. A 315, 185–194.

Banks, R.J., 1969. Geomagnetic variations and the electrical conductivity of the upper mantle. Geophys. J.R. Astron. Soc. 17, 457–487.

Berdichevsky, M.N., Vanyan, L.L., Kuznetsov, V.A., Levadny, V.T., Mandelbaum, M.M., Nechaeva, G.P., Okulessky, B.A., Shilovsky, P.P., Shpak, I.P., 1980. Geoelectric model of the Baikal region. Phys. Earth Planet. Inter. 22, 1–11.

Blohm, E.K., Worzyk, P., Scriba, H., 1977. Geoelectrical deep soundings in southern Africa using the Cabora Bassa power line. J. Geophys. 43, 665–679.

Booker, J.R., Chave, A.D., 1989. Introduction to the special section on the EMSLAB-Juan de Fuca Experiment. JGR 94, 14093–14098.

Calcagnile, G., 1982. The lithosphere–asthenosphere system in Fennoscandia. Tectonophysics 90, 19–35.

Calcagnile, G., 1991. Deep structure of Fennoscandia from fundamental and higher mode dispersion of Rayleigh waves. Tectonophysics 195, 139–149.

Calcagnile, G., Panza, G.F., 1987. Properties of the lithosphere–asthenosphere system in Europe with a view towards Earth conductivity. Pure Appl. Geophys. 125, 241–254.

Campbell, W.H., 1987. Introduction to electrical properties of the Earth's mantle. PAGEOPH 125, 193–204.

Constable, S.C., Duba, A., 1990. Electrical conductivity of olivine, a dunite, and the mantle. J. Geophys. Res. 95, 6967–6978.

Constable, S.C., McElhinny, M.W., McFadden, P.L., 1984. Deep schlumberger sounding and the crustal resistivity structure of central Australia. Geophys. J.R. Astron. Soc. 79, 893–910.

Constable, S.C., Parker, R.L., Constable, C.G., 1987. Occam's inversion: a practical algorithm for generating smooth models from electromagnetic sounding data. Geophysics 52, 289–300.

Constable, S., Shankland, T.J., Duba, A., 1992. The electrical

conductivity of an isotropic olivine mantle. J. Geophys. Res. 97, 3397–3404.

Cox, C.S., Constable, S.C., Chave, A.D., Webb, S.C., 1986. Controlled-source electromagnetic sounding of the oceanic lithosphere. Nature 320, 52–54.

Cull, J.P., 1985. Magnetotelluric soundings over a Precambrian contact in Australia. Geophys. J.R. Astron. Soc. 80, 661–675.

De Smet, J.H., Van den Berg, A.P., Vlaar, N.J., 1999. The evolution of continental roots in numerical thermo-chemical mantle convection models including differentiation by partial melting. Lithos 48, 153–170.

Duba, A.L., 1976. Are laboratory electrical conductivity data relevant to the Earth?. Acta Geodaet. Geophys. et Montanist. Acad. Sci. Hung. 11, 485–495.

Duba, A., Heard, H.C., Schock, R.N., 1974. Electrical conductivity of olivine at high pressure and under controlled oxygen fugacity. J. Geophys. Res. 79, 1667–1673.

Egbert, G.D., Booker, J.R., 1992. Very long period magnetotellurics at Tucson observatory: implications for mantle conductivity. J. Geophys. Res. 97, 15099–15112.

Filloux, J.H., 1973. Techniques and instrumentations for study of natural electromagnetic induction at sea. Phys. Earth Planet. Inter. 7, 323–338.

Fournier, H.G., Ward, S.H., Morrison, H.F. 1963. Magnetotelluric evidence for the low velocity layer. Space Sciences Lab., Univ. California Series No. 4, Issue No. 76.

Gamble, T.D., Goubau, W.M., Clarke, J., 1979. Magnetotellurics with a remote reference. Geophysics 44, 53–68.

Gough, D.I., 1987. Interim report on Electromagnetic Lithosphere–Asthenosphere Soundings (ELAS) to Co-ordinating Committee No. 5 of the International Lithosphere Programme. In: Fuchs, K., Froidevaux, C. (Eds.), Composition, Structure and Dynamics of the Lithosphere–Asthenosphere System, Amer. Geophys. Union Monograph, Geodynamics Series Vol. 16. Publ. 0135 of the Internatl. Lithosphere Program, pp. 219–237.

Haak, V., Hutton, V.R.S., 1986. Electrical resistivity in continental lower crust. In: Dawson, J.B., Carswell, D.A., Hall, J., Wedepohl, K.H. (Eds.), The Nature of the Lower Continental Crust. Geol. Soc. London, Spec. Publ., Vol. 24, pp. 35–49.

Hashin, Z., Shtrikman, S., 1963. A variational approach to the theory of the elastic behaviour of multiphase materials. J. Mech. Phys. Solids 11, 12–140.

Heikka, J., Zhamaletdinov, A.A., Hjelt, S.-E., Demidova, T.A., Velikhov, Ye.P., 1984. Preliminary results of MHD test registrations in northern Finland. J. Geophys. 55, 199–202.

Helmstaedt, H.H., Schulze, D.J., 1989. Southern African kimberlites and their mantle sample: implications for Archean tectonics and lithosphere evolution. In: Ross, J. (Ed.), Kimberlites and Related Rocks, Vol. 1: Their Composition, Occurrence, Origin, and Emplacement. Geol. Soc. Aust. Spec. Pub., Vol. 14, pp. 358–368.

Hoffman, P.F., 1990. Geological constraints on the origin of the mantle root beneath the Canadian shield. Phil. Trans. R. Soc. Lond. A 331, 523–532.

Hjelt, S.-E., Korja, T., 1993. Lithospheric and upper-mantle structures, results of electromagnetic soundings in Europe. Phys. Earth Planet. Inter. 79, 137–177.

Ji, S., Rondenay, S., Mareschal, M., Senechal, G., 1996. Obliquity between seismic and electrical anisotropies as a potential indicator of movement sense for ductile mantle shear zones. Geology 24, 1033–1036.

Jones, A.G., 1980. Geomagnetic induction studies in Scandinavia: I. Determination of the inductive response function from the magnetometer data. J. Geophys. 48, 181–194.

Jones, A.G., 1982. On the electrical crust–mantle structure in Fennoscandia: no Moho and the asthenosphere revealed?. Geophys. J.R. astron. Soc. 68, 371–388.

Jones, A.G., 1984. The electrical structure of the lithosphere and asthenosphere beneath the Fennoscandian shield. J. Geomagn. Geoelectr. 35, 811–827.

Jones, A.G., 1992. Electrical conductivity of the continental lower crust. In: Fountain, D.M., Arculus, R.J., Kay, R.W. (Eds.), Continental Lower Crust. Elsevier, Amsterdam, Chapter 3, pp. 81–143.

Jones, A.G., Gough, D.I., 1995. Electromagnetic studies in southern and central Canadian Cordillera. Can. J. Earth Sci. 3, 1541–1563.

Jones, A.G., Hutton, R., 1979b. A multi-station magnetotelluric study in southern Scotland: II. Monte-Carlo inversion of the data and its geophysical and tectonic implications. Geophys. J.R. Astron. Soc. 56, 351–368.

Jones, A.G., Olafsdottir, B., Tiikkainen, J., 1983. Geomagnetic induction studies in Scandinavia - III. Magnetotelluric observations. J. Geophys. 54, 35–50.

Jones, A.G, Ferguson, I.J., Grant, N., Roberts, B., Farquharson, C., 1997. Results from 1996 MT studies along SNORCLE profiles 1 and 1A. Lithoprobe Publication No. 56, pp. 42–47.

Jordan, T.H., 1988. Structure and formation of the continental tectosphere, J. Petrol., Special Lithosphere Issue pp. 11–37.

Kaikkonen, P., Pernu, T., Tiikainen, J., Nozdrina, A.A., Palshin, N.A., Vanyan, L.L., Yegorov, I.V., 1996. Deep DC soundings in southwestern Finland using the Fenno-Skan HVDC Link as a source. Phys. Earth Planet. Inter. 94, 275–290.

Karato, S., 1990. The role of hydrogen in the electrical conductivity of the upper mantle. Nature 347, 272–273.

Kharin, E.P., 1982. Study of the asthenospherie by deep electromagnetic sounding. ELAS report. Presented at Internat. Assoc. Geomagn. Aeron. Working Group I-3 meeting, Victoria, Canada, August.

Kohlstedt, D.L., Keppler, H., Rubie, D.C., 1996. Solubility of water in the alpha, beta and gamma phases of $(Mg,Fe)_2SiO_4$. Contrib. Mineral. Petrol. 123, 345–357.

Korja, T., 1993. Electrical conductivity distribution of the lithosphere in the central Fennoscandian shield. Precambrian Res. 64, 85–108.

Kosygin, Yu.A., Nikiforov, V.M., Al-perovic, M., Kononov, V.E., Kharakhinov, V.V., 1981. Electrical conductivity at depth in Sakhalin. Doklady Akademii Nauk SSSR 256, 1452–1455.

Krasnobayeva, A.C., D'yakonov, B.P., Astaf'yev, P.F., Batalova, O.V., Vishnev, V.S., Gavrilova, I.E., Zhuravleva, P.B., Kir-

illov, S.K., 1981. Structure of the northeastern part of the Baltic Shield based on magnetotelluric data. Izvestia (Earth Phys.) 17, 439–444.
Kurtz, R.D., Craven, J.A., Niblett, E.R., Stevens, R.A., 1993. The conductivity of the crust and mantle beneath the Kapuskasing uplift: electrical anisotropy in the upper mantle. Geophys. J. Int. 113, 483–498.
Kusky, T.M., 1993. Collapse of Archean orogens and the generation of late- to postkinematic granitoids. Geology 21, 925–928.
Lienert, B.R., 1979. Crustal electrical conductivities along the eastern flank of the Sierra Nevadas. Geophysics 44, 1830–1845.
Lilley, F.E.M., Woods, D.V., Sloane, M.N., 1981. Electrical conductivity from Australian magnetometer arrays using spatial gradient data. Phys. Earth Planet Inter. 25, 202–209.
Lizarralde, D., Chave, A., Hirth, G., Schultz, A., 1995. Northeastern Pacific mantle conductivity profile from long-period magnetotelluric sounding using Hawaii-to-California submarine cable data. J. Geophys. Res. 100, 17837–17854.
Madden, T.D., 1976. Random networks and mixing laws. Geophysics 41, 1104–1125.
Madden, T.D., 1983. Microcrack connectivity in rocks: a renormalization group approach to the critical phenomena of conduction and failure in crystalline rocks. J. Geophys. Res. 88, 585–592.
Mareschal, M., Kellett, R.L., Kurtz, R.D., Ludden, J.N., Bailey, R.C., 1995. Archean cratonic roots, mantle shear zones and deep electrical anisotropy. Nature 373, 134–137.
Maxwell, J.C., 1892. A Treatise on Electricity and Magnetism, 3rd. edn. (2). Clarendon Press, Oxford.
Moroz, Yu.F., 1985. A layer of increased electrical conductivity in the crust and upper mantle under Kamchatka. Izvestiya 21, 693–699.
Moroz, Yu.F., 1988. Deep geoelectric profile in the Asia-Pacific transition zone. Izvestiya 24, 383–386.
Nesbitt, B.E., 1993. Electrical resistivities of crustal fluids. J. Geophys. Res. 98, 4301–4310.
Olafsson, M., Eggler, D.H., 1983. Phase relations of amphibole, amphibole–carbonate, and phlogopite–carbonate peridotite: petrologic constraints on the asthenosphere. Earth Planet. Sci. Lett. 64, 305–315.
Oldenburg, D.W., Whittall, K.P., Parker, R.L., 1984. Inversion of ocean bottom magnetotelluric data revisited. J. Geophys. Res. 89, 1829–1833.
Olsen, N., 1998. The electrical conductivity of the mantle beneath Europe derived from C-responses from 3 to 720 h. Geophys. J. Int. 133, 298–308.
Osipova, I.L., Hjelt, S.-E., Vanyan, L.L., 1989. Source field problems in northern parts of the Baltic shield. Phys. Earth Planet. Inter. 53, 337–342.
Pavlenkova, N.I., Yegorkin, A.V., 1983. Upper mantle heterogeneity in the northern part of Eurasia. Phys. Earth Planet. Inter. 33, 180–193.
Polet, J., Anderson, D.L., 1995. Depth extent of cratons as inferred from tomographic studies. Geology 23, 205–208.
Praus, O., Pecova, J., Petr, V., Babuska, V., Plomerova, J., 1990. Magnetotelluric and seismological determination of the lithosphere–asthenosphere transition in Central Europe. Phys. Earth Planet. Inter. 60, 212–228.
Reiersol, O., 1950. Identifiability of a linear relation between variables which are subject to error. Econometrica 18, 375–389.
Ritz, M., 1984. Inhomogeneous structure of the Senegal lithosphere from deep magnetotelluric soundings. J. Geophys. Res. 89, 11317–11331.
Roberts, R.G., 1983. Electromagnetic evidence for lateral inhomogeneities within the Earth's upper mantle. Phys. Earth Planet. Inter. 33, 198–212.
Safonov, A.S., Bubnov, V.M., Sysoev, B.K., Chernyavsky, G.A., Chinareva, O.M., Shaporev, V.A., 1976. Deep magnetotelluric surveys of the Tungus Syneclise and on the West Siberian Plate. In: Adam, A. (Ed.), Geoelectric and Geothermal Studies. Akad. Kiado, Budapest, Hungary, 666–672.
Sato, H., Ida, Y., 1984. Low frequency electrical impedance of partially molten gabbro: the effect of melt geometry on electrical properties. Tectonophysics 107, 105–134.
Sato, H., Manghnani, M.H., Lienert, B.R., Weiner, A.T., 1986. Effects of electrode polarization on the electrical properties of partially molten rock. J. Geophys. Res. 91, 9325–9332.
Schmeling, H., 1985. Numerical models on the influence of partial melt on elastic, anelastic and electrical properties of rocks. Part I: Elasticity and anelasticity. Phys. Earth Planet. Inter. 41, 105–110.
Schmeling, H., 1986. Numerical models on the influence of partial melt on elastic, anelastic and electrical properties of rocks. Part II: Electrical conductivity. Phys. Earth Planet. Inter. 43, 123–136.
Schmucker, U., 1985. Electrical properties of the Earth's interior. In: Fuchs, K., Soffel, H. (Eds.), Numerical data and functional relationships in science and technology, Group V: IIb, Geophysics and Space Research, Springer-Verlag, Berlin, ISBN 3-540-12853-0, pp. 100-124.
Schock, R.N., Duba, A.G., Shankland, T.J., 1989. Electrical conduction in olivine. J. Geophys. Res. 94, 5829–5839.
Schultz, A., Kurtz, R.D., Chave, A.D., Jones, A.G., 1993. Conductivity discontinuities in the upper mantle beneath a stable craton. Geophys. Res. Lett. 20, 2941–2944.
Sclater, J.G., Jaupart, C., Galson, D., 1980. The heat flow through oceanic and continental crust and the heat loss of the earth. Rev. Geophys. Space Phys. 18, 269–311.
Senechal, G., Rondenay, S., Mareschal, M., Guilbert, J., Poupinet, G., 1996. Seismic and electrical anisotropies in the lithosphere across the Grenville Front. Can. Geophys. Res. Lett. 23, 2255–2258.
Shankland, T.J., Duba, A.G., 1990. Standard electrical conductivity of isotropic, homogeneous olivine in the temperature range 1200°C–1500°C. Geophys. Res. Internat. 103, 25–31.
Spence, A.G., Finlayson, D.M., 1983. The resistivity structure of the crust and upper mantle in the central Eromanga Basin, Queensland, using magnetotelluric techniques (Australia). J. Geol. Soc. Aust. 30, 1–16.
Tarits, P., 1986. Conductivity and fluids in the oceanic upper mantle. Phys. Earth Planet. Inter. 42, 215–226.
Thompson, P.H., Judge, A.S., Lewis, T.J., 1996. Thermal evolu-

tion of the lithosphere in the central Slave Province: Implications for diamond genesis, In: LeCheminant, A.N., Richardson, D.G., DiLabio, R.N.W., Richardson, K.A. (Eds.), Searching for Diamonds in Canada. Geol. Surv. of Canada, Open File 3228, pp. 151–160.

Tozer, D.C., 1972. The present thermal state of the terrestrial planets. Phys. Earth Planet. Inter. 6, 182–197.

Tozer, D.C., 1979. The interpretation of upper mantle electrical conductivities. Tectonophys. 56, 147–163.

Tyburczy, J.A., Roberts, J.J., 1990. Low frequency electrical response of polycrystalline olivine compacts; grain boundary transport. Geophys. Res. Lett. 17, 1985–1988.

Vanyan, L.L., 1984. Electrical conductivity of the asthenosphere. J. Geophys. 55, 179–181.

Vanyan, L.L., Berdichevsky, M.N., Fainberg, E.B., Fiskina, M.V., 1977. The study of the asthenosphere of the East European platform by electromagnetic sounding. Phys. Earth Planet. Inter. 14, P1–P2, Letter section.

Vanyan, L.L., Yegorov, I.V., Shilovsky, P.P., Al'perovich, I.M., Nikiforov, V.M., Volkova, O.V., 1983. Characteristics of deep electrical conductivity of northern Sakhlin. Izvestiya 19, 208–214.

Velikhov, Y.P., Zhamaletdinov, A.A., Belkov, I.V., Gorbunov, G.I., Hjelt, S.-E., Lisin, A.S., Vanyan, L.L., Zhdanov, M.S., Demidova, T.A., Korja, T., Kirillov, S.K., Kuksa, Y.I., Poltanov, A.Y., Tokarev, A.D., Yevstigneyev, V.V., 1986. Electromagnetic studies on the Kola peninsula and in northern Finland by means of a powerful controlled source. J. Geodyn. 5, 237–256.

Velikhov, Y.P., Zhdanov, M.S., Frenkel, M.A., 1987. Interpretation of MHD-sounding data from the Kola Peninsula by the electromagnetic migration method. Phys. Earth Planet. Inter. 45, 149–160.

Vidale, J.E., Ding, X.-Y., Grand, S.P., 1995. The 410-km-depth discontinuity: a sharpness estimate from near-critical reflections. Geophys. Res. Lett. 22, 2557–2560.

Vladimirov, N.P., 1976. Deep magnetotelluric surveys in the Baltic-Scandinavian Shield and the Kokchetav Block. In: Adam, A. (Ed.), Geoelectric and Geothermal Studies. Akad. Kiado. Budapest, Hungary, 615-616.

Watanabe, T., Kurita, K., 1993. The relationship between electrical conductivity and melt fraction in a partially molten simple system: Archie's law behavior. Phys. Earth Planet. Inter. 78, 9–17.

Watanabe, T., Kurita, K., 1994. Simultaneous measurements of the compressional-wave velocity and the electrical conductivity in a partially molten material. J. Phys. Earth. 42, 69–87.

Weidelt, P., 1972. The inverse problem of geomagnetic induction. Z. Geophys 38, 257–289.

Xu, Y., Poe, B.T., Shankland, T.J., Rubie, D.C., 1998. Electrical conductivity of olivine, wadsleyite and ringwoodite under upper-mantle conditions. Science 280, 1415–1418.